

# Improper, Blue-Shifting Hydrogen Bond between Fluorobenzene and Fluoroform<sup>†</sup>

Bernd Reimann,<sup>‡</sup> Konstantin Buchhold,<sup>‡</sup> Sascha Vaupel,<sup>‡</sup> Bernhard Brutschy,<sup>\*,‡</sup>  
Zdeněk Havlas,<sup>§,||</sup> Vladimír Špirko,<sup>||,⊥</sup> and Pavel Hobza<sup>\*,||,⊥</sup>

*Institut für Physikalische und Theoretische Chemie der J.W. Goethe-Universität Frankfurt, Marie-Curie-Strasse 11, 60439 Frankfurt am Main, Germany, Institute of Organic Chemistry and Biochemistry, Academy of Sciences of the Czech Republic, 166 10 Prague 6, Czech Republic, J. Heyrovsky Institute of Physical Chemistry, Academy of Sciences of the Czech Republic, 182 23 Prague 8, Czech Republic, and Center for Complex Molecular Systems and Biomolecules, 182 23 Prague 8, Czech Republic*

Received: October 11, 2000; In Final Form: January 9, 2001

Weakly bonded 1:1 complexes between fluorobenzene (Fb)/fluorobenzene-*d*<sub>5</sub> (Fb-*d*<sub>5</sub>) and fluoroform (Ff) were investigated spectroscopically by infrared ion-depletion spectroscopy (IR/R2PI) and theoretically by correlated ab initio methods. Their predissociation spectra exhibit an absorption comprised of two superimposed bands. These are blue-shifted by 12 and 21 cm<sup>-1</sup>, respectively, relative to the CH stretch of isolated fluoroform. Each IR band is assigned to a different hydrogen-bonded fluorobenzene·fluoroform isomer. The isomer with the most blue-shifted CH stretching vibration (21 cm<sup>-1</sup>) is assigned to a sandwich type structure, exhibiting a CH···π hydrogen bond. The cluster structures have been calculated by counterpoise- (CP-) corrected gradient optimization combined with anharmonic vibrational analysis using the CP-corrected Hessians. The predicted blue-shifts are 21 and 20.5 cm<sup>-1</sup> for the CH stretching frequencies of fluoroform upon formation of a sandwich and a planar structure, respectively. The theoretical and experimental shifts are thus well comparable. Natural bond orbital (NBO) analysis of the sandwich complex as well as analysis of the type and shape of the occupied molecular orbitals revealed the nature of the blue-shift. It is shown that the nature of the improper, blue-shifting H-bond in this complex differs from that in a common H-bond. While in the common XH···Y hydrogen bond the primary interaction is caused by an electron density transfer (EDT) from the electron donor Y to the antibonding orbitals of XH, leading to the red-shift and bond elongation in XH, the features of the improper, blue-shifting H-bond are due to secondary effects. In the sandwich complex the EDT takes place between the electron donor (π electron clouds of fluorobenzene) and the lone pairs of the fluorine atoms of fluoroform, leading to a structural reorganization of the fluoroform, including the contraction of the CH bond and a corresponding blue-shift of its CH stretching frequency. The NBO analysis as well as the analysis of the type and shape of the HOMO and HOMO-1 orbitals both elucidate the larger blue-shift for the sandwich-type isomer of the fluorobenzene·fluoroform cluster compared to the equivalent chloroform complex.

## 1. Introduction

Hydrogen-bonded (H-bonded) complexes belong to the most frequent intermolecular complexes and play a very important role in nature.<sup>1</sup> For example, they are responsible for the unique properties of liquid water as well as for the structures of most biomacromolecules. H-bonded complexes are stabilized mainly by electrostatic, induction, charge-transfer, and dispersion energy contributions. The singular properties of H-bonding also stem from the fact that all these terms contribute to the molecular interaction. None of them is dominant nor can any of them be neglected. Each energy term adds some important component to H-bonding; e.g., the electrostatic term gives the typical directionality, usually only slightly deviated from linearity. Many H-bonds are of the XH···Y type, where X is an electronegative atom and Y is either an electronegative atom having one or

more lone electron pairs or a region of excess electron density (e.g. π-electrons of aromatic systems). H-bonds having X = F, O, and N are the most common ones.<sup>2</sup> The concept of H-bonds was extended to CH···Y bonding, and both CH···electronegative atom as well as CH···π types of H-bonds have been observed.<sup>3</sup> The formation of a H-bond of the XH···Y type is accompanied by a weakening of the XH bond, which is manifested by the elongation of the XH bond with a concomitant decrease of the XH stretching frequency (the so-called red-shift). The red-shift of the XH stretching frequency is a characteristic feature of the formation of H-bonds.

Recently we found theoretically a new type of intermolecular bonding in carbon hydrogen donor complexes, which is characterized by the contraction of the CH bond and a blue-shift of the respective CH stretching frequency.<sup>4</sup> Because the spectroscopic manifestation of this new type of intermolecular bonding is opposite to the classical hydrogen bonds, we called it the “anti-H-bond”. This new type of H-bonding and its properties were confirmed experimentally in the fluorobenzene·chloroform (Fb·Cf) as well as the benzene·chloroform (Bz·Cf) complex using IR/R2PI infrared ion-depletion spectroscopy.<sup>5</sup> The calculated blue-shift<sup>5</sup> of the CH stretching frequency of chloroform agreed well with the experimental value of 14 cm<sup>-1</sup>.

<sup>†</sup> Part of the special issue “Edward W. Schlag Festschrift”.

<sup>‡</sup> Institut für Physikalische und Theoretische Chemie der J.W. Goethe-Universität Frankfurt.

<sup>§</sup> Institute of Organic Chemistry and Biochemistry, Academy of Sciences of the Czech Republic.

<sup>||</sup> Center for Complex Molecular Systems and Biomolecules.

<sup>⊥</sup> J. Heyrovsky Institute of Physical Chemistry, Academy of Sciences of the Czech Republic.

The proper theoretical description of this phenomenon requires the use of highly accurate theoretical methods including electron correlation, corrections of the basis set superposition error (BSSE), and anharmonic corrections. The BSSE can only be eliminated if the structure and frequencies are evaluated on the BSSE-corrected potential energy surfaces. We used the counterpoise<sup>5</sup> (CP) approximation to the BSSE and performed the CP-corrected gradient optimization and evaluated the CP-corrected Hessian matrices.

The term “anti-H-bond” was regarded to be misleading mainly because it contradicts the existence of a bond between both subsystems and also could mean the formation of a complex with antihydrogen. However, it has to be underlined that in “anti-H-bond” complexes we have formally the same type of bonding as in the classical hydrogen bond: the proton is placed between both subsystems and the stabilization of the complex is comparable. The manifestation of both types of H-bonds is, however, different (see above). Because the characteristic features are entirely opposite and, moreover, both types of H-bonds are of different origin (as shown later), we prefer the terms “H-bond” for the classical, red-shifting one and “improper, blue-shifting H-bond” for the original “anti-H-bond”.

A very large blue-shift of the CH stretching frequency was detected recently in the  $X^-\cdot H_3CY$  complexes ( $X = Cl, Y = Br; X, Y = I$ ), which were also thoroughly investigated theoretically.<sup>6</sup> Besides the intermolecular H-bonds also intramolecular H-bonds exist; these bonds are important for the structure of molecules. The intramolecular H-bonds are mostly studied in the liquid phase using NMR spin–spin X–H coupling constants. For classical H-bonds the X–H coupling decreases upon the formation of the intramolecular hydrogen bond. In several cases the increase of the coupling constant was detected. This phenomenon was studied in connection of the proximity effect (see the recent review of Contreras<sup>7</sup>).

In this paper we report on the experimental evidence and theoretical analysis of the improper, blue-shifting H-bond between fluoroform (Ff) and fluorobenzene (Fb)/fluorobenzene- $d_5$  (Fb- $d_5$ ). The objectives of our study are 3-fold:

- (i) find an experimental proof for the existence of the complex and the improper H-bond by detecting the blue-shift of the CH stretching frequency;
- (ii) describe theoretically the structure and properties of the complex;
- (iii) understand the origin and nature of the improper H-bond in the complex fluorobenzene·fluoroform.

To obtain a deeper insight into the nature of the improper H-bond a natural bond orbital (NBO) analysis as well as the analysis of the type and shape of highest occupied molecular orbitals of the complex will be performed. Let us recall that the NBO analysis of H-bonding has shown the importance of electron density transfer (EDT) from the proton acceptor to the proton donor,<sup>8</sup> in particular from the lone electron pairs of the proton acceptor Y to XH antibonding orbitals of the proton donor. An increase of the electron density in a XH antibonding orbital results in a XH bond elongation accompanied by a red-shift of the XH stretching frequency.

## 2. Experiment

**2.1. Experimental Setup.** Fb/Ff ( $C_6H_5F/CHF_3$ ) and Fb- $d_5$ /Ff ( $C_6D_5F/CHF_3$ ) clusters have been investigated experimentally using resonant two-photon ionization (R2PI) and IR/R2PI ion depletion spectroscopy. These methods have been described in more detail elsewhere.<sup>9,10</sup> Briefly, the molecular clusters are produced in a pulsed supersonic expansion of a mixture of 0.3%

Ff and 0.05% Fb in He. The clusters are ionized by a frequency doubled dye laser via one-color-R2PI (1C-R2PI). The cations are mass analyzed in a reflectron-time-of-flight mass spectrometer (RETOF-MS). The ion signals are digitized in a transient recorder (LeCroy TR8828C) programmed in a multiboxcar mode. By virtue of the resonant excitation and the nonresonant ionization step of R2PI, the yield of a specific ion reflects the UV absorption spectrum of its neutral precursor and is termed in the following R2PI spectrum. Usually a neutral cluster precursor exhibits a characteristic fingerprint spectrum. Thus a particular cluster size can be investigated by tuning the UV laser to a cluster-specific absorption frequency in its R2PI spectrum. The vibrational spectrum of such a cluster is recorded by scanning the wavelength of a “hole burning” infrared laser and by monitoring the yield of the ion. The IR light pulse precedes the UV-probe pulse by about 70  $\mu s$ . If the wavelength of the IR pulse hits resonantly a vibration of a cluster, it will predissociate within nanoseconds if the vibrational energy exceeds the binding energy of the cluster. These ion depletion spectra, monitored by R2PI, are henceforth termed IR/R2PI spectra. The IR light is generated by a tunable, injection-seeded optical parametric oscillator (OPO) using  $LiNbO_3$  crystals.<sup>11</sup> Only the idler beam is utilized and passed antiparallel into the molecular beam. Its spectral bandwidth is 0.2  $cm^{-1}$ , and its pulse energy in the CH stretch region is 5 mJ. The absolute wavelength is checked regularly by a wavemeter (Atos LM007). The spectra are averaged over 100 laser shots in a waveform digitizer and processed in a personal computer. To improve the signal-to-noise ratio five individual spectra are averaged and smoothed.

Fb (99% purity) was purchased from Fluka, Fb- $d_5$  from Aldrich (97%), and Ff from Lancaster (98%). All chemicals are used without further purification.

**2.2. Experimental Results and Discussion.** *Fb/Ff.* The R2PI spectra of the cluster systems investigated are presented in Figure 1. That of the  $Fb^+\cdot Ff$  mass channel is displayed in Figure 1a. It shows a nearly symmetric, unusual broad UV band 1 (fwhm: 180  $cm^{-1}$ ), the maximum of which is blue-shifted by 223  $cm^{-1}$  relative to the  $S_1 \leftarrow S_0$   $0_0^0$  transition of Fb ( $\nu_{00} = 37818$   $cm^{-1}$ ). The  $Fb^+\cdot(Ff)_2$  mass channel exhibits a similar broad band (band 2), now blue-shifted by 296  $cm^{-1}$  (Figure 1b). In the  $Fb^+\cdot(Ff)_n$  mass channels with  $n > 2$ , the signals appear at nearly the same spectral position as band 2 (not shown).

Neither UV band 1 nor 2 can be attributed to a single cluster species. Band 1 (223  $cm^{-1}$ ) shows a small shoulder on its blue side, which we assign to contributions from 1: $n$  clusters with  $n \geq 2$ . Comparing the IR/R2PI spectra obtained from different positions within band 1, one can evaluate the part where larger clusters contribute to the signal by fragmentation (hatched area in Figure 1a). We found out that at the maximum of band 1 the  $Fb^+\cdot Ff$  ion signal originates mainly from the 1:1 cluster (contributions of larger clusters are less than 10%).

The corresponding IR/R2PI spectrum is presented in Figure 2a. It is assigned to the Fb·Ff cluster. It should be noted that this vibrational spectrum was nearly independent from the wavelength of the R2PI laser when varied over the part of the excitation profile assigned to the 1:1 clusters. The IR/R2PI spectrum obtained by probing on the blue side of band 1 (not shown) is contaminated by fragmentation of larger 1: $n$  clusters with  $n \geq 2$ . At 296  $cm^{-1}$  this contribution to the  $Fb^+\cdot Ff$  signal from larger clusters rises to about 30%. The IR/R2PI ion depletion spectrum obtained from band 2 (296  $cm^{-1}$ ) of the  $Fb^+\cdot(Ff)_2$  mass channel is shown in Figure 2b. It is indistin-

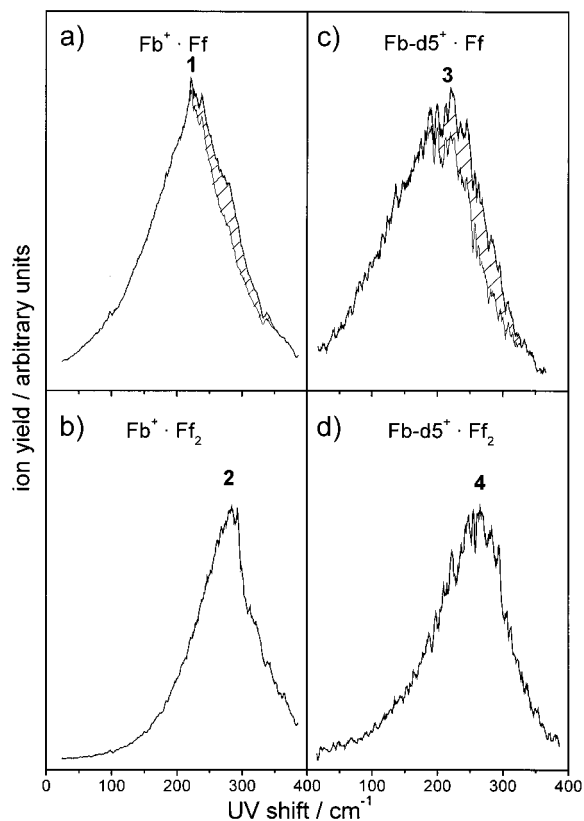


**Figure 1.** R2PI-spectra of  $\text{Fb}^+\cdot\text{Ff}_{1,2}$  and  $\text{Fb-d}_5^+\cdot\text{Ff}_{1,2}$ . The shifts are given relative to the  $S_1 \leftarrow S_0 0_0^0$  transitions of Fb ( $\nu_{00} = 37818 \text{ cm}^{-1}$ ) and  $\text{Fb-d}_5$  ( $\nu_{00} = 37985 \text{ cm}^{-1}$ ), respectively. The contributions from fragmenting larger clusters to the signals in the  $\text{Fb}^+\cdot\text{Ff}$  and  $\text{Fb-d}_5^+\cdot\text{Ff}$  mass channels are hatched. Experimental parameters: stagnation pressure of the gas mixture 5.5 bar; nozzle diameter  $500 \mu\text{m}$ ; UV energy about  $60 \mu\text{J/pulse}$ .

guishable from the depletion spectra of  $\text{Fb}^+\cdot(\text{Ff})_{n \geq 2}$  masses probed at the same UV frequency. From this we conclude that the IR/R2PI spectrum shown in Figure 2b constitutes a superposition of the spectra of larger 1:n clusters. Therefore, the R2PI band 2 cannot be assigned solely to the 1:2 cluster. By comparing these R2PI spectra with those of similar clusters such as  $\text{Fb}\cdot(\text{Cf})_n^5$  and  $\text{Bz}\cdot(\text{Ff})_n^{12}$ , one finds that in all cases the  $S_1 \leftarrow S_0 0_0^0$  transitions of the 1:1 clusters show a smaller blue-shift than the 1:2 clusters. A possible explanation is that the attachment of a second solvent molecule on the opposite side of the aromatic ring results in an additional polarization, which increases the blue-shift of the electronic transition. A third solvent molecule presumably has no direct contact to the aromatic ring; therefore, the UV shift changes only little. The extended fragmentation prevents the distinction of the spectrum of the  $\text{Fb}\cdot(\text{Ff})_2$  cluster from those of the larger clusters. In the following we will therefore only discuss the  $\text{Fb}\cdot\text{Ff}$  spectrum (Figure 2a).

The IR spectrum of isolated Fb has been studied in the gas phase by Lipp and Seliskar.<sup>13</sup> Absorptions corresponding to the CH stretching fundamentals  $\nu_{20a}$ ,  $\nu_2$ ,  $\nu_{7b}$ , and  $\nu_{13}$  could be assigned unambiguously. In liquid phase also the  $\nu_{20b}$  fundamental was observed, which is missing in the gas-phase spectra. Therefore we took the liquid-phase value of the  $\nu_{20b}$  mode for comparison.<sup>14</sup>

The IR/R2PI spectrum in Figure 2a shows five relatively sharp absorption bands. Assuming that the energetic order of the aromatic CH modes is not changed by a relatively weak interaction with the solvent, they can be assigned to the aromatic

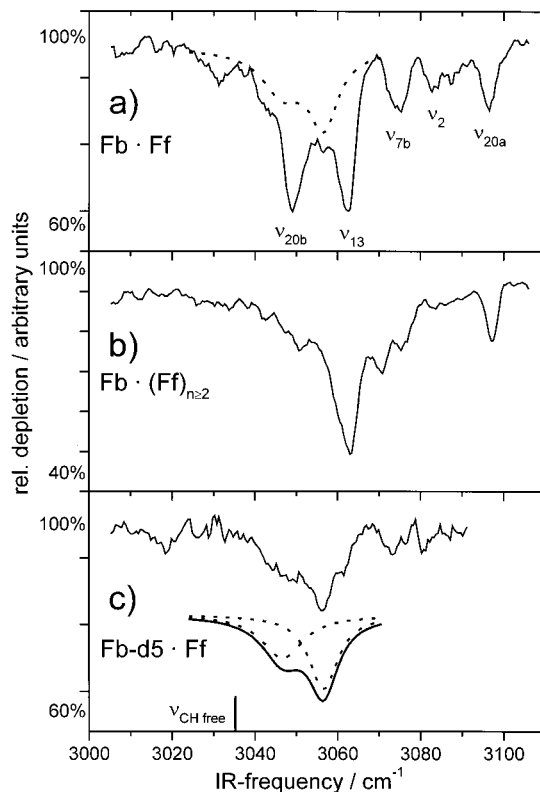


**Figure 2.** IR/R2PI-spectra of (a)  $\text{Fb}\cdot\text{Ff}$ , (b)  $\text{Fb}\cdot(\text{Ff})_{n \geq 2}$ , and (c)  $\text{Fb-d}_5\cdot\text{Ff}$ . The aromatic CH fundamentals in (a) are assigned correspondingly to Lipp and Seliskar.<sup>13</sup> The dotted line in (a) is the fit to the Ff CH band from  $\text{Fb-d}_5\cdot\text{Ff}$ . The fit to the CH absorption band is given in (c) below the experimental spectrum. The deconvoluted Lorentz profiles are shown in dotted lines. The CH absorption of Ff in the gas phase at  $3035 \text{ cm}^{-1}$  is marked below.

**TABLE 1: Experimental Absorption Frequencies of the 1:1 Complexes (in  $\text{cm}^{-1}$ )**

vibration	Fb gas phase <sup>13</sup>	Fb·Ff		Fb·Cf	
		abs	rel	abs	rel
$\nu_{20b}^{14}$	3049.0	3049.0	0.0		
$\nu_{13}$	3061.0	3062.5	1.5	3059.5	-1.5
$\nu_{7b}$	3069.5	3075.0	5.5	3070.5	1.0
$\nu_2$	3080.0	3083.0	3.0	3079.0	-1.0
$\nu_{20a}$	3094.0	3096.0	2.0	3092.5	-1.5
		FF gas phase <sup>15</sup>		Fb·Cf	
$\nu_{\text{CH}}$ (isomer I)	3035	3056.5	21.5	3047	14
$\nu_{\text{CH}}$ (isomer II)		3047	12.0		

CH stretching fundamentals of Fb. The absolute frequencies and the shifts relative to those in the isolated Fb are given in Table 1. Except for the  $\nu_{20b}$  mode, which is not shifted, all other modes show a slight blue-shift. This spectrum differs remarkably from that obtained for the  $\text{Fb}\cdot\text{Cf}$  complex.<sup>5</sup> There the  $\nu_{20b}$  mode is not observed, and the CH stretching frequencies show red-shifts of  $3.5 \pm 0.5 \text{ cm}^{-1}$  relative to the corresponding bands of  $\text{Fb}\cdot\text{Ff}$ .

Having assigned the prominent IR absorption bands to the CH vibrations of the Fb monomer, one must identify the CH vibrational mode of Ff. Since apart from the five absorptions just assigned no additional absorption band appears, one has to assume that the CH mode of Ff overlaps with the CH stretching bands of Fb. Clear indications for this superposition are visible in the spectrum: While the  $\nu_{20a}$ ,  $\nu_2$ , and  $\nu_{7b}$  modes of Fb are rather narrow and weak in intensity and probably are not overlapped by other bands, the low-frequency modes  $\nu_{20b}$  and

$\nu_{13}$  show a pronounced line intensity and broadening. A contribution from an underlying CH stretch of Ff can therefore be suspected. To verify this assumption the IR/R2PI spectra from Fb- $d_5$ /Ff clusters were recorded. The isotope substitution in the Fb removes the interference of the aromatic CH stretches, since the CD fundamentals of Fb- $d_5$  are found between 2250 and 2300  $\text{cm}^{-1}$ .<sup>13</sup> Therefore the IR/R2PI spectrum from the Fb- $d_5$ /Ff clusters taken in the region above 3000  $\text{cm}^{-1}$  should be only due to the CH absorption of Ff.

*Fb- $d_5$ /Ff.* The  $S_1 \leftarrow S_0$   $0_0^0$  electronic transition in Fb- $d_5$  is found at 37 985  $\text{cm}^{-1}$ . This spectral position corresponds to a isotopic blue-shift of 167  $\text{cm}^{-1}$  relative to the corresponding transition in Fb. The R2PI bands of the Fb- $d_5$ ·(Ff) $_n$  clusters are shifted similarly as for nondeuterated species. The shapes of the UV bands obtained from the deuterated and nondeuterated Fb·(Ff) $_n$  clusters are practically identical (Figure 1a–d).

The IR/R2PI spectrum obtained from band 3 (Figure 2c) shows an unusually broad and asymmetric absorption between 3039 and 3066  $\text{cm}^{-1}$ , with the maximum located at 3056  $\text{cm}^{-1}$ . Since only Ff possesses a CH group in this complex, its assignment is unambiguous. The unusual shoulder on the red side of the band suggests a superposition of two absorption bands. Hence we deconvoluted it by two Lorentzian profiles. The resulting two bands (shown as dotted lines in Figure 2c) appear at 3047 and 3056.5  $\text{cm}^{-1}$ , respectively, with an intensity ratio of 1:2.5. We assign them to two different isomers.

The assumption of two different isomers necessitates some additional remarks on the observed R2PI spectrum. Its large spectral width of 180  $\text{cm}^{-1}$  is quite unusual for such small clusters. For comparison that of benzene·Ff shows two sharp and distinct bands rising up from a congested, underground (due to fragmenting larger clusters), while that of Fb·Cf shows long, spectrally resolved progressions of low-frequency intermolecular modes ( $\Delta\nu = 7\text{--}8$   $\text{cm}^{-1}$ ), extending over a spectral range of 75  $\text{cm}^{-1}$ .<sup>12</sup> The excitation of such progressions in the  $S_1$  state of a complex is indicative of a large geometrical change of the equilibrium structure upon the electronic excitation. The low-frequency modes would be typical of a floppily bound cluster. Hence it seems likely that similar progressions account for the surprising broadness of the R2PI spectrum of Fb·Ff. This assumption would be in consonance with the large UV shift of 223  $\text{cm}^{-1}$  observed for this spectrum. The fact that no vibrational pattern appears could be due to the superposition of similarly broad spectra of two different isomers. This would also explain why the observed CH modes, assigned to two different isomers, could not be isolated spectroscopically by changing the wavelength of the ionization laser. Therefore these results might be regarded as an example that, even in the case of spectrally congested R2PI spectra, the vibrational spectra, recorded in the fingerprint region of the cluster(s) in the  $S_0$  state, may exhibit a clear signature of its structure(s).

In a comparison of the widths of the aromatic CH stretches of the Fb·Ff cluster (5–8  $\text{cm}^{-1}$ ) with those observed for the similar 1:1 cluster with chloroform (2–3  $\text{cm}^{-1}$ )<sup>5</sup>, they are also broadened. This may be a further indication of the overlap of the IR spectra of two different isomers.

From this spectroscopic assignment, the two isomers for the Fb·Ff cluster may be characterized by the following spectral features: The one with the most intense absorption (isomer I) exhibits a CH stretching mode which is blue-shifted by about 21.5  $\text{cm}^{-1}$  relative to that in isolated Ff (3035  $\text{cm}^{-1}$ ),<sup>15</sup> while the aromatic CH frequencies are blue-shifted between 0 and 5  $\text{cm}^{-1}$ . The CH mode of Ff of the second isomer (isomer II) exhibits a blue-shift of 12  $\text{cm}^{-1}$ .

A structural assignment of the isomers from the shift of the CH vibration alone is not possible. However for the Bz·Ff cluster, where no second isomer exists, one finds a single-line spectrum with a similar blue-shift of 25  $\text{cm}^{-1}$ . Since in this case a sandwich-type structure, stabilized by a H-bond between the CH group and the  $\pi$ -electron system, is most probable, we similarly assign isomer I to a  $\text{CH}\cdots\pi\cdots\text{H}$ -bonded structure. The isomer II, displaying a shift of 12  $\text{cm}^{-1}$ , can be assigned to an isomer with a planar structure. The simultaneous presence of both isomers in the supersonic beam indicates that they possess comparable binding energies.

The ab initio calculations, discussed in the following, also predict the existence of two isomeric cluster structures: one where the Ff is H-bonded by its CH group to the aromatic  $\pi$ -system and another where the CH group is H-bonded to the fluorine atom of Fb.

### 3. Calculations

All ab initio calculations were performed at the second-order Møller–Plesset (MP2) level, which covers a significant part of the correlation energy, at two different basis sets, 6-31G\* and 6-31++G\*\*. The structures of both monomers and the 1:1 cluster were determined using a gradient optimization on either BSSE uncorrected or BSSE corrected potential energy surfaces. In the former case the BSSE was included a posteriori by applying the Boys–Bernardi counterpoise method<sup>16</sup> and also the deformation energy was considered. In the later case the BSSE corrections, again using the CP method, were applied not only to the energy calculations but also to the gradients of energy<sup>17,18</sup> and the BSSE was eliminated at each optimization cycle. This procedure inherently includes the deformation energy. The CP-uncorrected procedure is not accurate since it does not consider the CP-correction effects on the geometry and vibrational frequencies. The standard gradient optimization was considered converged if the gradient norm was lower than 0.0003 au; for CP-corrected gradient optimization the limit was 0.0006 au.

Also the harmonic vibrational frequencies have been evaluated for the optimal structures found by the standard as well as CP-corrected optimizations, in the latter case using the CP-corrected Hessians.

To take the anharmonic effects into account, we performed one-dimensional anharmonic calculations. The CH bonds are treated as independent oscillators, and all other (intermolecular and intramolecular) coordinates are optimized using a CP-corrected gradient optimization. The coupling with other coordinates is effectively covered via ab initio optimization of the 1:1 structures for a selected set of the CH distances. The energies of the optimized molecular geometries were quantitatively fitted to the following power expansion:

$$V(r_{\text{CH}}) = \sum F_i [1 - \exp\{-a(r_{\text{CH}} - r_e)\}]^i \quad (1)$$

Here  $r_{\text{CH}}$  is the CH internuclear separation,  $r_e$  is the appropriate equilibrium bond length, and  $F_i$  and “ $a$ ” are the fitting parameters. The required CH stretch fundamental frequencies are obtained as differences of the first-excited- and ground-state vibrational energies of the corresponding one-dimensional Schrödinger equation for the following Hamiltonian:

$$H = -\hbar^2/2\mu + V(r_{\text{CH}}) \quad (2)$$

Here  $\hbar$  is the Planck constant and  $\mu$  is the reduced mass of the C–H fragment.

**TABLE 2: Stabilization Energies (in kcal/mol), Geometry (in Å), and Vibration Characteristics (in  $\text{cm}^{-1}$ ) of Sandwich and Planar Structures of the  $\text{Fb}\cdots\text{Ff}$  Complex Evaluated at Standard and CP-Corrected PES with Various Basis Sets**

structure <sup>b</sup>	PES	$\Delta E$		$\Delta r^a$		$\Delta \nu^a$
		MP2/6-31G*	MP2/6-31++G**	MP2/6-31G*	MP2/6-31++G**	MP2/6-31G*
Sandwich	std	1.57	2.06	-0.0065	-0.0031	38
	CP-corr	2.25	2.38 <sup>c</sup>	-0.0023	-0.0019	31
Planar	std	1.42	2.28	-0.0029 (-0.0006)	0.0023	51 (14)
	CP-corr	1.69	2.30	-0.0019 (0.0)	0.0019	34

<sup>a</sup>  $\Delta r$  and  $\Delta \nu$  concern CH bond and CH stretch frequency in Ff; numbers in parentheses refer to the CH bond in Fb. <sup>b</sup> Cf. Figure 3. <sup>c</sup> Minimum gradient norm achieved equals to 0.016 au.

The natural bond orbital analysis<sup>19</sup> was performed using the MP2 electron density. Care should be paid to different terminologies. The antibonding NBO orbital must not be confused with the virtual MO of the MO theory since the latter is strictly unoccupied. The NBO antibonding orbitals exhibit nonzero occupancy and contribute to the total energy. NBO delocalization effects discussed above for H-bonding are associated with  $n-\pi^*$  interactions between filled (Y) and unfilled (XH) orbitals. Reed et al.<sup>8</sup> described these interactions as being of charge-transfer type. However, the authors warn that this term should not be confused with Mullikens's treatment of charge-transfer complexes. To avoid this confusion we use throughout the paper the term electron density transfer which describes the transfer of NBO electron density from occupied natural orbitals of the proton acceptor to natural orbitals of the proton donor. It is to be mentioned that NBO analysis performed with the Hartree-Fock electron density yields results qualitatively similar to that with the MP2 electron density; this is an argument supporting the use of the occupied MOs determined from Hartree-Fock calculations for the molecular orbital analysis. To eliminate the basis set extension effects the NBO analysis of monomers was performed using the basis set of the 1:1 complex (with the proper amount of the ghost atoms).

All the calculations were done using the GAUSSIAN 98 code<sup>20</sup> and our own program<sup>18</sup> for CP-corrected optimization and Hessian evaluation (using Gaussian 98 as a generator of the first and second energy derivatives).

#### 4. Theoretical Results and Discussion

The first step in the theoretical study of the fluorobenzene-fluoroform complex was the investigation of the potential energy surface. For the present complex two different structures were considered, a sandwich (stacked) structure having a  $\text{CH}\cdots\pi$  contact and a planar structure with one or two  $\text{CH}\cdots\text{F}$  contacts. The structures found by standard as well as CP-corrected gradient optimizations are similar (Figure 3), and the respective energies, geometry parameters, and vibration characteristics are collected in Table 2.

First, the standard gradient optimization results are mentioned. While the 6-31G\* calculations prefer the sandwich structure over the planar one, the opposite result is obtained when extending the basis set to 6-31++G\*\*. The planar structure is by about 0.2 kcal/mol more stable than the sandwich one. The energy differences obtained for both structures at the 6-31G\* and 6-31++G\*\* levels are, however, small.

The more reliable CP-corrected gradient optimizations gave unambiguous answers concerning the relative stability of both structures. At both levels the sandwich structure is more stable than the planar one. The energy difference calculated at the 6-31G\* level is 0.56 kcal/mol in favor of the sandwich complex, while at the 6-31++G\*\* level the energies are comparable (0.08 kcal/mol). The convergence of the CP-corrected optimization is generally very slow, necessitating a large number of gradient

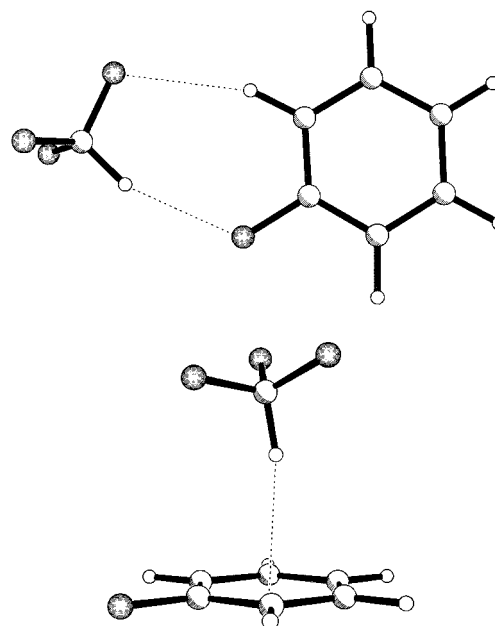


**Figure 3.** Structures of the  $\text{Fb}\cdot\text{Ff}$  complexes found by standard and CP-corrected gradient optimization.

calculations. In the case of CP-corrected gradient optimization of the sandwich structure at the MP2/6-31++G\*\* level we were not able to reduce the gradient norm below the value of 0.016 au. The obtained stabilization energy (2.38 kcal/mol) represents therefore a lower bound, and the actual stabilization energy should be larger by an unknown amount. The sandwich structure of the  $\text{Fb}\cdot\text{Ff}$  complex thus corresponds to the global minimum and the planar structure to a local one. However, the energy difference between both structures is small and both structures should coexist in a supersonic beam. We are aware of the fact that performing calculations at higher theoretical level (larger basis set and larger fraction of correlation energy) might change the ordering of complex isomers. However, the CP-corrected optimization exhibits faster convergence to complete basis set limit than standard optimization.

An interesting effect was found for the planar structure of the complex possessing two  $\text{CH}\cdots\text{F}$  contacts (see Figure 3). Both CH bond lengths were reduced upon complex formation. This reduction is larger for the CH bond of Ff (cf. Table 2). A contraction of both bond lengths is accompanied by a blue-shift of both CH stretch frequencies which is again larger for the CH stretch of Ff. This finding is fully supported by experimental data (see above).

In the sandwich complex the CH bond length of Ff is contracted upon complex formation (cf. Table 2). This contraction is larger for a standard gradient optimization and a smaller basis set. The contraction of the CH bond is accompanied by the increase of the CH stretch frequency, i.e., by the blue-shift of this frequency. The blue-shift obtained by the standard

**TABLE 3: Comparison of Theoretical and Experimental Characteristics of the Fb·Ff and Fb·Cf Complexes (Theoretical Results Calculated at the MP2/6-31G\* Level)**

cluster	$\Delta E^a$ std	CP-corr	$\Delta\nu^b$ std	CP-corr	exp
Fb·Ff <sup>c</sup>	1.6, 1.4	2.2, 1.7	38, 51	31, 34	21, 12
Fb·Cf <sup>d</sup>	2.5	3.1	67	21	14

<sup>a</sup> Stabilization energy of the complex (in kcal/mol). <sup>b</sup> Change of CH stretch frequency upon complex formation (in  $\text{cm}^{-1}$ ). <sup>c</sup> Sandwich and planar structures. <sup>d</sup> Sandwich structure; results taken from ref 5.

calculation is larger than with the CP-corrected one. The differences in the blue-shifts of the CH stretches in the sandwich and planar structure are larger in calculations with standard optimization; more reliable CP-corrected (harmonic) calculations yield a small difference of  $3 \text{ cm}^{-1}$  in favor of the sandwich structure. The same tendency was found previously for the corresponding complex with chloroform, i.e., for Fb·Cf<sup>5</sup> (cf. Table 3). The standard, CP-uncorrected, calculation predicted a blue-shift of  $67 \text{ cm}^{-1}$  for the sandwich structure of the Fb·Cf complex, which was reduced to  $21 \text{ cm}^{-1}$  when CP-corrected calculations were performed.

The CP-corrected calculations predict blue-shifts of 31 and  $34 \text{ cm}^{-1}$  for the CH stretch frequencies of the Ff upon formation of the sandwich and planar structures, respectively, of the Fb·Ff complex. Because the CH vibration (as well as other vibrational modes) is anharmonic we should go beyond the limits of the harmonic approximation. With performance of one-dimensional anharmonic calculations on the basis of the CP-corrected potential energy surface, the calculated blue-shifts for the sandwich and planar structures were reduced to 20.5 and  $21 \text{ cm}^{-1}$ . These values nicely agree with the experimental results of 21 and  $12.5 \text{ cm}^{-1}$ . The present level of theory is, however, unable to explain the small difference of  $8 \text{ cm}^{-1}$  for the second shift.

The Fb·Ff complex (studied presently) and Fb·Cf complex<sup>5</sup> were investigated at the same theoretical level (CP-corrected optimization and harmonic vibrational analysis on the basis of CP-corrected Hessians), which gives the chance to compare the theoretical characteristics of both clusters and also compare theoretical with experimental data (Table 3). The Fb·Cf complex is more stable than Fb·Ff, and the same difference in the stabilization energy is found between the standard and CP-corrected levels. However, the relative values of the blue-shifts evaluated at the standard and CP-corrected level differ. Standard level calculations predicted a larger blue-shift for the Fb·Cf complex while CP-corrected calculations give a larger blue-shift for the Fb·Ff complex. The experimental results unambiguously support the CP-corrected values (cf. Table 3). This is a strong argument supporting the use of CP-corrected gradient optimization and CP-corrected Hessians.

#### Nature of Improper H-Bonding in the Fb·Ff Complex.

Results of NBO analysis performed using the MP2 electron density for both structures of the complex are summarized in Table 4. From the table it is evident that in both structures there is an EDT from Fb to Ff. In the case of the sandwich structure 4 me (millielectrons) are transferred from Fb to Ff; this transfer is slightly smaller for the planar structure (2.4 me). Further, the same orbitals are involved in EDT of both isomers. The value of EDT is sensitive to the optimization procedure — in the case of standard gradient optimization (instead of CP-corrected optimization) the EDT is reduced from 4.0 to 2.8 me. The largest part of this EDT goes to the lone electron pairs of all fluorine atoms, and there is no EDT to the CH region. The increase of electron density in fluorine lone pairs results in a structural reorganization of the CHF<sub>3</sub> subsystem, specifically

**TABLE 4: Electron Density Transfer<sup>a</sup> (EDT) from NBO Analysis for Sandwich and Planar Structures of the Fb·Ff Complex Evaluated at CP-Corrected PES (MP2/6-31G\*)**

structure <sup>b</sup>		sandwich	planar
Fb <sup>c</sup>	$\Sigma\text{C}-\text{C}^d$	-0.9	-0.9
	$\Sigma\text{C}-\text{H}^e$	-0.5	-0.6
Ff <sup>c</sup>	C-F <sup>f</sup>	-0.1	0.2
	C-H <sup>*g</sup>	-0.1	0.1
	$\Sigma\text{LP F}^h$	3.3	2.3
tot. EDT (Fb → Ff)		4.0	2.4

<sup>a</sup> In millielectrons. Subsystems are treated in the dimer basis set. The difference between the sum of the components and the total EDT is due to many small contributions. <sup>b</sup> Cf. Figure 3. <sup>c</sup> Change upon complexation. <sup>d</sup>  $\sigma$  and  $\pi$  C-C orbitals. <sup>e</sup>  $\sigma$  C-H orbitals. <sup>f</sup>  $\sigma$  C-F orbitals. <sup>g</sup>  $\sigma^*$  C-H orbital. <sup>h</sup> Lone pairs in all fluorine atoms.

(in the case of sandwich structure) the following: (i) The H-C-F angles increase in the average by  $0.2^\circ$ . (ii) The CF bonds are elongated in the average by  $1.8 \text{ m}\text{\AA}$ . (iii) The CH bond is contracted by  $2.3 \text{ m}\text{\AA}$ . If all geometrical changes in fluoroform are considered, the harmonic vibrational analysis for this deformed structure results in the blue-shift of  $28 \text{ cm}^{-1}$  of the CH stretch frequency with respect to the CH frequency in the fully optimized fluoroform. This means that the largest part of the overall blue-shift of  $31 \text{ cm}^{-1}$  calculated at the harmonic level (cf. Table 2) is due to the structural reorganization of fluoroform and the rest is due to the polarization of fluoroform by fluorobenzene. Any attempt to explain the blue-shift of the CH stretching frequency of fluoroform by only one type of structural change failed: (i) By considering the opening of the H-C-F angles only and by optimizing the rest of Ff, a negligible blue-shift of the CH stretch frequency ( $\sim 3 \text{ cm}^{-1}$ ) is obtained. (ii) By elongating the CF bond lengths only and optimizing the rest of Ff, we obtained also a similar negligible blue-shift.

Therefore, we can conclude this part by stating that the blue-shift of the CH stretch frequency of Ff is due to the a structural reorganization of the Ff, which results from an electron density transfer to the fluorine atoms. The primary effect is thus the EDT to the fluorine atoms, which subsequently leads to the structural reorganization of Ff, including the contraction of the CH bond. This conclusion is important since in the classical H-bonds of XH...Y type the primary effect is due to EDT to the antibonding orbital of the XH bond. The increase of electron density in this orbital results in the elongation of the XH bond.

For comparison we present the results of the NBO analysis for the structurally similar benzene·H<sub>2</sub>O sandwich complex possessing the OH... $\pi$  H-bond (the OH bond was fixed at the C<sub>6</sub> axis of the benzene molecule). NBO analysis at the MP2/6-31G\* level yields a EDT of 4.8 me from benzene to water. The dominant part (4.2 me) of the EDT goes into the OH  $\delta^*$  antibonding orbital directed to the  $\pi$ -system of benzene and only 0.5 me to the other OH bond. An increase of electron density in the OH antibonding orbital results in the elongation of this OH bond.

Also the smaller blue-shift in the Fb·Cf complex, possessing a larger stabilization energy and a larger amount of EDT than in the case of the Fb·Ff complex, can be explained on the basis of the NBO analysis. Contrary to the Fb·Ff complex where a dominant part of EDT is directed to the fluorine atoms, in the Fb·Cf complex the enhanced electron density (6.1 me; CP-corrected gradient optimization) is distributed almost equally among all atoms of the chloroform (hydrogen Rydberg orbital, 2.3 me; lone pair orbitals of two chlorine atoms,  $2 \times 1.4 \text{ me}$ ; CCl antibonding orbital, 0.9 me; CH antibonding orbital, 0.8

me). The increase of electron density at the chlorine atoms and in the CCl antibonding orbitals induces a structural reorganization in the Cf including the CH contraction. On the other hand the increase of electron density in the CH antibonding orbital and in the hydrogen Rydberg orbital leads to the elongation of the CH bond. The final net effect is the contraction of the CH bond which is, however, smaller than in the case of Fb•Ff. Let us finally remind that neither the stabilization energy nor the amount of EDT correlates with the magnitude of the blue-shift in both complexes, which provides evidence about the complex character of the binding.

Analyzing the type and shape of the highest occupied (HF, canonical) MOs of the Fb•Ff and Fb•Cf sandwich complexes, we found important differences. In the case of the former complex the HOMO and HOMO-1 orbitals are almost exclusively localized at Fb and the lone electron pairs of the fluorine atoms. In the case of the complex with chloroform the HOMO contains part located on Fb, chlorine lone pairs, and CCl orbitals and also a CH antibonding orbital of chloroform. Let us finally mention that the HOMO-2 MO is considerably lower in energy for both complexes.

The improper, blue-shifting H-bond has some features similar to those of a standard H-bond and some completely different. The similar features, which justify the use of the term "H-bond", are the following: (i) The hydrogen is placed between X and Y (in the sense of  $XH\cdots Y$ ). (ii) The electron density is transferred from the proton acceptor (Y) to the proton donor (XH). (iii) The stability and directionality are similar. The different features, which support the use of the term "improper, blue-shifting" are the following: (i) The formation of the improper H-bond leads to a strengthening of the XH bond and not to its weakening as in the case of the classical H-bond. (ii) Upon complex formation the CH bond is contracted and CH stretching frequency exhibits a blue-shift. (iii) The electron density is not transferred to the XH region but to the remote part of the proton donor, which results in its structural reorganization.

## 5. Conclusion

The weak complexes of fluorobenzene•fluoroform and fluorobenzene-*d*<sub>5</sub>•fluoroform were investigated using the IR/R2PI ion-depletion spectroscopy. From the experimental results it was found that the fluoroform CH frequency was shifted to a higher frequency by 21 and 12 cm<sup>-1</sup>, respectively (blue-shift), upon complexation; the larger blue-shift was assigned to the sandwich-type structure, and the smaller one, to the planar structure of the complex.

On the basis of a CP-corrected gradient optimization we demonstrated that fluorobenzene forms a sandwich-type and a planar complex with fluoroform. The CH bond of fluoroform is contracted upon complex formation (both in the sandwich and planar structure), and its stretching frequency is blue-shifted by 31 and 34 cm<sup>-1</sup>. Taking anharmonic corrections into account, these shifts are reduced to 21 and 20.5 cm<sup>-1</sup>. These values agree well with the experimental results. The relative values of the blue-shifts in fluorobenzene•fluoroform and fluorobenzene•chloroform determined experimentally are reproduced only if the CP-corrected gradient optimization combined with anharmonic vibrational analysis using CP-corrected Hessians is

applied. On the basis of the NBO analysis using the MP2 electron density, it was shown that the dominant part of the electron density transfer from fluorobenzene is directed to the fluorine atoms of fluoroform and none to the CH region. The structural reorganization of fluoroform, which results from this EDT to the fluorine lone pairs, is responsible for the blue-shift of the CH stretching frequency. The improper, blue-shifting H-bond in the complex studied is thus a secondary effect, while in the classical (red-shifted) H-bonds it is the primary effect.

**Acknowledgment.** The financial support provided from the Center for Complex Molecular Systems and Biomolecules, Czech Republic (project LN00A032 of MSMT CR), from the J.W. Goethe Universität Frankfurt, and from the "Fonds der Chemischen Industrie" is acknowledged. We also gratefully acknowledge CPU time on the NEC-SX4 at CHMI Prague (Grant No. LB98202, project Infra2 of MSMT CR) and at the Rechenzentrum der Universität Stuttgart (RUS) (Grant No. 11738).

## References and Notes

- (1) Hobza, P.; Zahradník, R. *Intermolecular Complexes*; Elsevier: Amsterdam, 1988.
- (2) Scheiner, S. *Hydrogen Bonding*; Oxford University Press: New York, 1997.
- (3) Desiraju, G. R.; Steiner, T. *The Weak Hydrogen Bond*; Oxford University Press: Oxford, U.K., 1999.
- (4) Hobza, P.; Špirko, V.; Selzle, H. L.; Schlag, E. W. *J. Phys. Chem. A* **1999**, *102*, 2501.
- (5) Hobza, P.; Špirko, V.; Havlas, Z.; Buchhold, K.; Reimann, B.; Barth, H.-D.; Brutschy, B. *Chem. Phys. Lett.* **1999**, *299*, 180.
- (6) Weber, J. M.; Kelley, J. A.; Robertson, W. H.; Lisle, K. M.; Ayotte, P.; Johnson, M.; Havlas, Z.; Hobza, P. *J. Am. Chem. Soc.* **2000**, submitted for publication.
- (7) Contreras, R. H.; Peralta, J. E.; Giribet, C. G.; Ruit de Azúa, M. C.; Facelli, J. C. *Annu. Rep. NMR Spectrosc.* **2000**, *41*, 55.
- (8) Reed, A. E.; Curtiss, L. A.; Weinhold, F. *Chem. Rev.* **1988**, *88*, 889.
- (9) Brutschy, B. *Chem. Rev.* **1992**, *92*, 1567.
- (10) Djafari, S.; Lembach, G.; Barth, H.-D.; Brutschy, B. *Z. Phys. Chem.* **1996**, *195*, 253.
- (11) Huisken, F.; Kulcke, A.; Voelkel, D.; Laush, C.; Lisy, J. M. *Appl. Phys. Lett.* **1993**, *62*, 805.
- (12) Reimann, B.; Buchhold, K.; Vaupel, S.; Brutschy, B. *Z. Phys. Chem.* **2001**, in print.
- (13) Lipp, E. D.; Seliskar, C. J. *J. Mol. Spectrosc.* **1978**, *73*, 290.
- (14) Josien, M. L.; Labas, J. M. *Bull. Soc. Chim. Fr.* **1956**, *53*, 57.
- (15) Dübal, H. R.; Quack, M. *J. Chem. Phys.* **1984**, *81*, 3779.
- (16) Boys, S. F.; Bernardi, F. *Mol. Phys.* **1970**, *19*, 553.
- (17) Simon, S.; Duran, M.; Danneberg, J. J. *J. Chem. Phys.* **1996**, *105*, 11024.
- (18) Hobza, P.; Havlas, Z. *Theor. Chem. Acc.* **1998**, *99*, 372.
- (19) Foster, J. P.; Weinhold, F. *J. Am. Chem. Soc.* **1980**, *102*, 7211. Reed, A. E.; Weinhold, F. *J. Chem. Phys.* **1983**, *78*, 1736, 4066. Reed, A. E.; Weinstock, R. B.; Weinhold, F. *J. Chem. Phys.* **1985**, *83*, 735 as well as ref 8.
- (20) Frisch, M. J.; Trucks, G. W.; Schlegel, H. B.; Scuseria, G. E.; Robb, M. A.; Cheeseman, J. R.; Zakrzewski, V. G.; Montgomery, J. A., Jr.; Stratmann, R. E.; Burant, J. C.; Dapprich, S.; Millam, J. M.; Daniels, A. D.; Kudin, K. N.; Strain, M. C.; Farkas, O.; Tomasi, J.; Barone, V.; Cossi, M.; Cammi, R.; Mennucci, B.; Pomelli, C.; Adamo, C.; Clifford, S.; Ochterski, J.; Petersson, G. A.; Ayala, P. Y.; Cui, Q.; Morokuma, K.; Malick, D. K.; Rabuck, A. D.; Raghavachari, K.; Foresman, J. B.; Cioslowski, J.; Ortiz, J. V.; Baboul, A. G.; Stefanov, B. B.; Liu, G.; Liashenko, A.; Piskorz, P.; Komaromi, I.; Gomperts, R.; Martin, R. L.; Fox, D. J.; Keith, T.; Al-Laham, M. A.; Peng, C. Y.; Nanayakkara, A.; Gonzalez, C.; Challacombe, M.; Gill, P. M. W.; Johnson, B.; Chen, W.; Wong, M. W.; Andres, J. L.; Gonzalez, C.; Head-Gordon, M.; Replogle, E. S.; Pople, J. A. *Gaussian 98, Revision A.7*; Gaussian, Inc.: Pittsburgh, PA, 1998.